forests

MDPI

Article

Low Tree-Growth Elasticity of Forest Biomass Indicated by an Individual-Based Model

Robbie A. Hember [1,*] and Werner A. Kurz [2]

[1] Climate Change and Integrated Planning Branch, BC Ministry of Forests, Lands, Natural Resource Operations and Rural Development, 727 Fisgard Street, Victoria, BC V8W9C5, Canada
[2] Pacific Forestry Centre, Canadian Forest Service, Natural Resources Canada, 506 West Burnside Road, Victoria, BC V8Z1M5, Canada; Werner.Kurz@canada.ca
* Correspondence: Robert.Hember@gov.bc.ca; Tel.: +1-250-882-4715

Received: 25 November 2017; Accepted: 4 January 2018; Published: 6 January 2018

Abstract: Environmental conditions and silviculture fundamentally alter the metabolism of individual trees and, therefore, need to be studied at that scale. However, changes in forest biomass density (Mg C ha^{-1}) may be decoupled from changes in growth (kg C year^{-1}) when the latter also accelerates the life cycle of trees and strains access to light, nutrients, and water. In this study, we refer to an individual-based model of forest biomass dynamics to constrain the magnitude of system feedbacks associated with ontogeny and competition and estimate the scaling relationship between changes in tree growth and forest biomass density. The model was driven by fitted equations of annual aboveground biomass growth (G_{ag}), probability of recruitment (P_r), and probability of mortality (P_m) parameterized against field observations of black spruce (*Picea mariana* (Mill.) BSP), interior Douglas-fir (*Pseudotsuga menziesii* var. *glauca* (Beissn.) Franco), and western hemlock (*Tsuga heterophylla* (Raf.) Sarg.). A hypothetical positive step-change in mean tree growth was imposed half way through the simulations and landscape-scale responses were then evaluated by comparing pre- and post-stimulus periods. Imposing a 100% increase in tree growth above calibrated predictions (i.e., contemporary rates) only translated into 36% to 41% increases in forest biomass density. This corresponded with a *tree-growth elasticity* of forest biomass ($\varepsilon_{G,SB}$) ranging from 0.33 to 0.55. The inelastic nature of stand biomass density was attributed to the dependence of mortality on intensity of competition and tree size, which decreased stand density by 353 to 495 trees ha^{-1}, and decreased biomass residence time by 10 to 23 years. Values of $\varepsilon_{G,SB}$ depended on the magnitude of the stimulus. For example, a retrospective scenario in which tree growth increased from 50% below contemporary rates up to contemporary rates indicated values of $\varepsilon_{G,SB}$ ranging from 0.66 to 0.75. We conclude that: (1) effects of warming and increasing atmospheric concentrations of carbon dioxide and reactive nitrogen on biomass production are greatly diminished, but not entirely precluded, scaling up from individual trees to forest landscapes; (2) the magnitude of decoupling is greater for a contemporary baseline than it is for a pre-industrial baseline; and (3) differences in the magnitude of decoupling among species were relatively small. To advance beyond these estimates, studies must test the unverified assumptions that effects of tree size and stand competition on rates of recruitment, mortality, and growth are independent of climate change and atmospheric concentrations of carbon dioxide and nitrogen.

Keywords: tree growth; forest biomass density; tree-growth elasticity; individual-based model; forest growth enhancement; forest growth decline

1. Introduction

With a residence time ranging from decades to centuries [1–3], tree biomass in forest ecosystems is a large and relatively volatile reservoir in the global carbon cycle. Biomass-dense forest ecosystems,

including natural old-growth and intensively managed plantations, also hold a wide range of socio-economic values. Given the magnitude of environmental changes projected by global climate models, long-term plans to maintain and regrow new biomass-dense forests need to better understand how ongoing environmental changes will influence forest biomass density.

There is a common assumption in carbon cycle science that global change factors, including rising concentrations of atmospheric carbon dioxide, reactive nitrogen, and air temperature, have increased the rate of tree growth [4–6]. Although a few recent studies of stand-level forest biomass production support the assumption that growth enhancement is widespread in humid boreal and temperate forests [7–11], it remains unclear whether growth enhancement is increasing the amount of carbon that is stored in trees, or whether it may be accelerating the rate at which carbon cycles through the forest biomass reservoir.

Global change factors influence the metabolism of individual trees and studies must, therefore, focus on estimating changes at that scale. For example, the expectation that global change factors have increased tree growth is rooted in many confirmatory experiments performed on individual trees [12–18]. However, changes in the growth rate of individual trees can trigger many feedback responses, involving the ontogeny of trees, intensity of competition for resources, and succession, which may then decouple changes in forest biomass from tree growth enhancement [19–21].

Negative feedbacks are widely recognized. For example, summarizing experimental responses of trees to carbon dioxide enrichment, Körner [22] argued for differentiating between responses of "uncoupled" and "expanding" systems that have not yet reached normal resource constraints and steady-states of foliage and fine roots, and "fully coupled" systems that have reached these states. Drawing on the relationship between the growth and longevity of trees, Bugmann and Bigler [19] argued that any significant change in the growth rate of individual trees, caused by a rising carbon dioxide concentration for example, would likely be offset by negative system feedbacks at the scale of forest ecosystems.

Specific dynamics are also quantitatively understood. For example, the strong dependence between average tree size and stand density has led to a general rule describing the carrying capacity of forest ecosystems [23]. The rule is sometimes applied to predict density-dependent mortality in models [24]. In a phase of self-thinning, the rule suggests that increases in the average body size of survivors must be accompanied by a decrease in stand density. Any increase or decrease in the growth rate of trees translates into a predictable change in population, as it should accelerate the increase in average body size (attained at any age) and simply accelerate the rate at which trees succumb to competition. Overwhelmingly, these relationships are understood within the context of natural stand dynamics, yet available field studies suggest that the rule may apply equally to systems experiencing long-term time trends in growth [11].

Many empirical studies also report the 'U-shaped' dependence of tree mortality on tree size [25–29], while the absolute growth rate of individual trees tends to peak at an intermediate tree size [25,30,31]. The size-dependence of mortality and growth are emergent properties that likely involve varying degrees of immobilization of nutrients with time since disturbance, decreasing hydraulic conductance with an increasing path length of the vascular system, increasing exposure to wind, anatomical changes with age, and antecedent effects of past injury (e.g., [32–35]). The resulting size-dependence of growth and mortality must influence the longevity and maximum size of survivors, which in turn must contribute to the overall biomass storage capacity of forest ecosystems [25].

Although observation networks provide the ability to analyze responses at the scale of individual trees and small field plots, forest ecosystem models are generally needed to understand how demographics and growth vary and how they affect biomass dynamics across a broader spatial and temporal scale [25,36]. This can be achieved with a wide range of individual-based models, including Growth and Yield models, Gap models, process-based models, and hybrid models [37–40]. Despite the prevalence of such models, few studies have documented the magnitude of negative

feedback responses to changes in tree growth and the scaling relationship between tree growth and forest biomass density.

In this study, we assessed how changes in tree growth translated into changes in stand biomass density across forest landscapes. To achieve this, we analyzed predictions from an individual-based model of forest biomass, *Sawtooth*, that integrates the dependencies of recruitment, mortality and growth on tree size, age, and the intensity of stand competition. To gain a broad perspective of the scaling relationships across boreal and temperate forests, we chose three species that vary widely in average forest biomass density. Research questions were addressed by testing the hypotheses that: (1) the dependence of recruitment, mortality, and growth on tree size and stand competition would collectively cause negative feedback responses to changes in tree growth, acting to decouple changes in forest biomass density from changes in tree growth; (2) the relationship between changes in tree growth and forest biomass density would be independent of the magnitude of the growth stimulus and; (3) across species, the magnitude of decoupling would increase with initial biomass density, reflecting the greater starting intensity of competition.

2. Data and Methods

2.1. Forest Inventory Data

Trees identified as black spruce (*Picea mariana* (Mill.) BSP), interior Douglas-fir (*Pseudotsuga menziesii* var. *glauca* (Beissn.) Franco), or western hemlock (*Tsuga heterophylla* (Raf.) Sarg.) were compiled from databases provided by agencies in British Columbia, Alberta, Saskatchewan, Manitoba, Ontario, New Brunswick, Nova Scotia, Newfoundland and Labrador, and the United States (Figure 1).

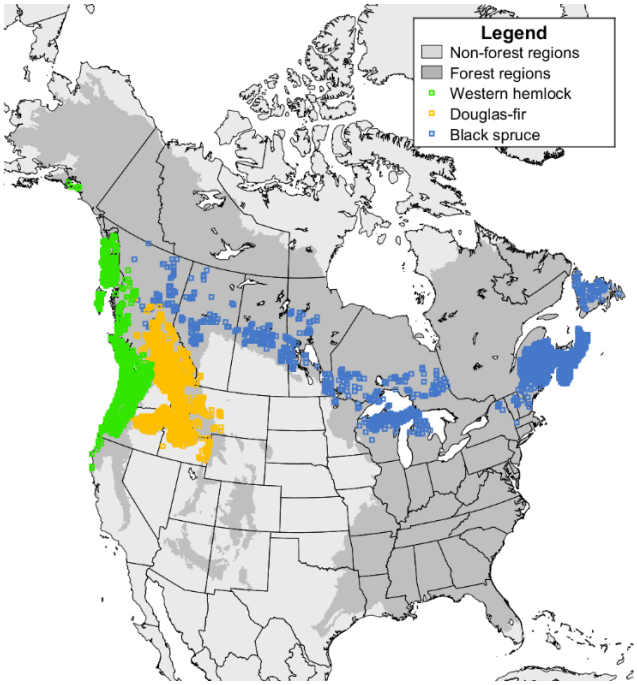

Figure 1. Map of field plots that contributed to the calibration of equations of growth, mortality, or recruitment.

Interior Douglas-fir was differentiated from the coastal variety by only including trees east of the Cascade/Coastal Mountain range. At each field plot, a census was taken for trees exceeding a threshold breast-height diameter. The lowest observations of breast-height diameter were below 5.0 cm with the exceptions of Saskatchewan and Newfoundland and Labrador, which only considered trees with a breast-height diameter greater than 7.1 and 9.1 cm, respectively. Between 1% to 5% of the

samples were affected by some form of management and these observations were excluded from the samples. The biomass of bark, branches, foliage, and stemwood was calculated from dimension analysis based on diameter and height [41,42]. Total aboveground biomass was then calculated from the summation of foliage, branches, bark, and stemwood. All values of biomass were converted to the mass of carbon assuming a carbon-dry wood ratio of 0.5 [43].

The final samples included between 5779 and 8206 field plots (Table 1). Sampling was conducted between the 1960's and 2010's and targeted stands that were between 10 and 190 years old. On average, black spruce, interior Douglas-fir, and western hemlock were representative of continental, cold-temperate, and maritime-temperate climates, respectively. Referencing estimates of warm-season mean soil water content from a monthly surface water balance model suggested that all species covered large ranges in hydrological conditions, but that the sample of interior Douglas-fir was, on average, substantially drier than the other two species.

Table 1. Descriptive statistics of the field plot samples.

Statistic	Black Spruce	Interior Douglas-Fir	Western Hemlock
Num. plots	8206	5779	8024
Num. observations	304,850	335,518	436,053
Time 1st percentile	1965	1962	1947
Time mean	1992	1986	1982
Time 99st percentile	2012	2015	2013
MAT 1st percentile	−3.4	1.3	3.4
MAT mean	1.8	5.2	8.0
MAT 99st percentile	6.9	8.8	10.5
Wws 1st percentile	45	8	65
Wws mean	175	59	163
Wws 99st percentile	200	183	200
SA 1st percentile	10	24	11
SA mean	71	74	45
SA 99st percentile	173	185	190

MAT: mean annual temperature (°C); W_{ws}: warm-season soil water content (mm); SA: stand age (years).

Statistical modelling was conducted for three dependent variables. The first dependent variable was the periodic mean annual aboveground biomass growth rate of individual trees, G_{ag} (kg C tree^{-1} year^{-1}). Growth was calculated from the annualized difference between estimates of tree biomass at sequential census dates. By measuring a wide range of stand ages, the observations of growth included trees that eventually succumb to density-dependent mortality, yet the growth of trees during a period in which trees died was not measured due to uncertainty in the year that the tree died. The second dependent variable was the annual probability of recruitment, P_r (% year^{-1}), which was inferred from a binary variable describing whether the tree was a recruit (a value of "1") or not (a value of "0") during the measurement interval. The third dependent variable was the annual probability of mortality, P_m (% year^{-1}), which was inferred from a binary variable describing whether the tree died (a value of "1") or not (a value of "0") during the measurement interval.

Independent variables included the aboveground biomass of individual trees at the first measurement date, B_{ag} (kg C tree^{-1}); stand age at the first measurement date, SA (years); biomass of all trees in the plot at the first measurement date, SB (Mg C ha^{-1}); and biomass of larger trees in the plot at the first measurement date, SBLT (Mg C ha^{-1}). Stand age was either supplied by the data source, or estimated from the subsample of trees that were measured at each plot. The biomass of larger trees was calculated by summing the product of aboveground biomass of individual trees and area expansion factors for individuals with a greater biomass than the focal tree.

2.2. Modelling

A function, *Sawtooth*, was written in Matlab (MATLAB R2016a, The Mathworks Inc., Natick, MA, USA) to calculate the mass balance of trees for $i = 1 \ldots m$ annual time-intervals and $j = 1 \ldots n$ homogeneous spatial units (i.e., stands), each with an area of 10000 m^2. The biomass dynamics of each stand were ultimately driven by equations describing the recruitment, growth, and mortality of trees. The two defining features of each equation are: (1) the sample of field observations that the equations were calibrated against (e.g., typically representing a specific combination of tree species and region); and (2) the specification of the equations. For this study, we focused on calibrating and applying relatively simple equations for each species, herein called "Default 1" equations, with the intention of representing basic patterns of ontogeny, aging, and competition among trees. The Default 1 equations intentionally avoided additional complexity and, thus, provide a high-bias/low variance alternative to equations that attempt to represent additional system complexity [26,30].

Stand-level variables were initialized as $m \times n$ (stand-level) matrices. For each stand, the model tracked the vital status and growth rate of $k = 1 \ldots SD_{max}$ trees by initializing a second set of intermediate $m \times SD_{max}$ matrices for each variable. The value, SD_{max}, specified the maximum possible number of live trees per spatial unit, or stand density (SD). As such, there were SD_{max} spaces (with an area of $SD_{max}/10{,}000$ m^2) available where a live tree could exist. If SD_{max} is set high enough, the balance between predicted recruitment and mortality rates will yield a steady-state value of stand density that never reaches SD_{max}. Each tree in the tree-level matrix was randomly assigned a species according to prescribed fractions of each initial species.

During the first time-interval, all SD_{max} spaces were initially classified as "empty" and then $l = 1 \ldots N_{seed}$ were randomly selected to germinate. The status of these germinating trees was converted to "live tree", and the aboveground biomass of the germinating trees was converted to a low value, $B_{ag,seed}$. The values of $B_{ag,seed}$ were drawn randomly from a normal distribution with the mean, $B_{ag,seed,mu}$, and standard deviation, $B_{ag,seed,sig}$, and were constrained by $B_{ag,seed} > 0$. Hence, a degree of within-stand variation in germination rates was assumed to lead to an initial cohort of trees with a biomass that follows a normal distribution at the end of the first time-interval.

For each stand, the model looped through $i = 2 \ldots m$ time-intervals. First, trees that were "live" at the end of the previous time-interval were identified and used to calculate the stand-level explanatory variables required to predict recruitment, growth, and mortality for that time-interval. This included stand age (SA), aboveground biomass density (SB_{ag}), and aboveground biomass of larger trees ($SBLT_{ag}$). Stochastic processes during each time-interval were controlled by vectors of random numbers drawn from a uniform distribution between 0 and 1 for all spaces inhabited by live trees (r_{live}) and empty spaces (r_{empty}).

Models of tree recruitment predict the number of trees that surpass a specified tree size threshold, and range from simply applying a constant probability, to dynamic models that predict responses to varying stand conditions [44–47]. Overall, modelling recruitment generally requires separate predictions of occurrence and frequency. Here, the strategy was to treat species occurrence as a boundary condition—an assumption made by the user that a seed source of the focal species exists, or was predicted to occur using established models within stand, j [48–51]. In instances where the focal species occurs, logistic regression was used to predict the annual probability of recruitment of the k^{th} tree:

$$P_{r,k} = \frac{\exp(logit(P_{r,k}))}{1 + \exp(logit(P_{r,k}))} \quad (1)$$

We assumed that the most simplistic version of a dynamic recruitment model would consider dependence on the intensity of stand competition. To represent this type of dynamic model, the Default 1 equation was defined as:

$$logit(P_{r,k}) = a_0 + a_1 SB_{ag} \quad (2)$$

where a_0 and a_1 are fixed effects. (See the previous paragraph for a definition of explanatory variables.) The equations were calibrated against ungrouped samples of each species. The logistic regression equations were fitted against observations of ingrowth; the sample consisted of trees that were counted at both the first and second measurement dates ("0" or "not a recruit") and trees that were not counted at the first measurement date, but surpassed the threshold tree size for inclusion between the first and second measurement dates ("1" or "recruit"). As SD is constrained by SD_{Max}, the probability of recruitment is only calculated and applied to the available empty spaces, by comparing P_r(empty) with the r_{empty}. For any trees with P_r(empty) > r_{empty}, the status of the empty space was converted from "empty" to "live tree", the age of the recruited tree was converted to one year, and the aboveground biomass of the recruited tree was converted to $B_{ag,seed}$.

Whereas many comparable models predict the annual increments of diameter and height before deriving the growth rate of stemwood volume or biomass, Sawtooth assumes aboveground biomass growth as the dependent variable [30]. For this study, estimates of aboveground biomass growth were derived from dimension analysis of the tree diameter and height using Canada's national biomass equations [42] and a dry weight-to-carbon ratio of 0.5 [43]. The Default 1 equation predicted the natural logarithm of the aboveground biomass growth of the k^{th} tree as:

$$\ln\left(G_{ag,k}\right) = b_0 + b_1 \ln\left(B_{ag,k}\right) + b_2 B_{ag,k} + b_3 SA_k + b_4 SBLT_{ag} + b_5 SB_{ag} \quad (3)$$

where $b_0 \ldots b_5$ are fixed effects. By including $\ln(B_{ag,k})$ and $B_{ag,k}$, the equation has the flexibility to represent an optima in the size-dependence of growth [30,31,52,53]. By including $SBLT_{ag}$ and SB_{ag}, the equation has the flexibility to represent relative and absolute expressions of the intensity of stand competition. Predictions of aboveground biomass growth are then added to the existing aboveground biomass of live trees.

The annual probability of tree mortality (P_m) was calculated as the sum of simulated and prescribed mortality. Simulated mortality was inferred from statistical models (e.g., logistic regression). Prescribed mortality provided the flexibility to also utilize observations of discrete disturbance events derived from forest inventory and monitoring systems. The detection strength and prediction accuracy of tree mortality observation systems are often highly specialized and, therefore, unevenly distributed across the complete spectrum of landscape-scale tree mortality. To simultaneously accommodate data sources of varying specialization, simulated and prescribed types of mortality were further partitioned into non-stand-replacing and stand-replacing components:

$$P_m = \max(P_{m,SimNSR}, P_{m,SimSR}, P_{m,PreNSR}, P_{m,PreSR}) \quad (4)$$

where $P_{m,SimNSR}$ is simulated non-stand-replacing mortality, $P_{m,SimSR}$ is simulated stand-replacing mortality, $P_{m,PreNSR}$ is prescribed non-stand-replacing mortality, and $P_{m,PreSR}$ is prescribed stand-replacing mortality. As the landscapes in the present study were hypothetical, we relied on a combination of $P_{m,SimNSR}$ and $P_{m,SimSR}$ to represent the total rates of tree mortality, while prescribed disturbance events, $P_{m,PreSR}$ and $P_{m,PreNSR}$, were set to zero.

$P_{m,SimNSR}$ represents lethal processes in the high-frequency/low-magnitude part of the landscape mortality spectrum; this is the frequent occurrence of low rates of mortality within intact stands, commonly referred to as 'background' or 'regular' mortality. The processes that are represented by $P_{m,SimNSR}$ will depend on the specification of the equations and quality of the sample that it was calibrated against. Technically, there is nothing stopping $P_{m,SimNSR}$ from predicting 100% mortality in rare cases. As with recruitment, we used logistic regression to predict $P_{m,SimNSR}$ of the k^{th} tree, defining the Default 1 equation as:

$$logit(P_{m,SimNSR,k}) = c_0 + c_1 B_{ag,k} + c_2 {B_{ag,k}}^2 + c_3 SA_k + c_4 SBLT_{ag} + c_5 SB_{ag} \quad (5)$$

where $c_0 \ldots c_5$ are fixed effects. By design, the Default 1 equation of mortality focuses on representing effects of ontogeny, aging, and competition on mortality rates. The equation is underspecified because it does not include many other factors that contribute to overall rates of mortality observed at field plots, including wind, insects, pathogens, weather, animals, and pollutants [27,54]. To some unknown extent, these factors partially contribute to the average of predictions, but failure to specify them in the model (due to difficulties in measuring them) likely introduces bias in the predictions. Nevertheless, the Default 1 equation tests fundamental constraints on the longevity of trees that are central to biomass dynamics of intact stands. Upon the calculation of Equation (5), mortality counts were tallied according to the number of trees with $P_{\mathrm{m,SimNSR}}(\mathrm{live}) > r_{\mathrm{live}}$. The status of the trees that died were converted from "live" to "empty", and the age and aboveground biomass of the trees that died were converted to zero.

The model also accounted for lethal processes that operate in the low-frequency/high magnitude part of the landscape mortality spectrum by simulating stand-replacing mortality as:

$$P_{\mathrm{m,SimSR}} = \max(P_{\mathrm{m,SimSR,H}}, P_{\mathrm{m,SimSR,F}}, P_{\mathrm{m,SimSR,I}}, P_{\mathrm{m,SimSR,P}}) \quad (6)$$

where $P_{\mathrm{m,SimSR,H}}$ is mortality caused by harvesting, $P_{\mathrm{m,SimSR,F}}$ is mortality caused by fire, $P_{\mathrm{m,Sim\ SR,I}}$ is mortality caused by insects, and $P_{\mathrm{m,SimSR,P}}$ is mortality caused by pathogens. To represent landscape-scale forest biomass dynamics, it was essential to impose stand-replacing disturbance in this study, yet the study did not strongly depend on the specific nature of the disturbance regime. Across all time-intervals and all stands, stand-replacing disturbance was represented by assuming a constant fire return interval of $\mathrm{RI_{Fire}}$ = 200 years, corresponding to $P_{\mathrm{m,SimSR,F}}$ = 0.005. Other stand-replacing disturbances were not considered, setting $P_{\mathrm{m,SimSR,H}}$, $P_{\mathrm{m,SimSR,I}}$, and $P_{\mathrm{m,SimSR,P}}$ to 0.0.

Upon completing the time-intervals of each stand, the aboveground biomass of each tree was partitioned into foliage, bark, branches, and stemwood based on species-specific allometric equations [42]. The belowground biomass for each tree was derived from aboveground biomass based on allometric equations for coniferous trees [55]. Belowground biomass was partitioned into coarse and fine roots based on allometric relationships [55,56]. Total tree biomass was then calculated as the sum of foliage, branches, bark, stemwood, coarse roots, and fine roots. Biomass turnover of foliage, bark, branches, coarse roots, and fine roots, τ_{F}, τ_{Bk}, τ_{Br}, τ_{Rc}, and τ_{Rf}, respectively, were calculated based on constant rate coefficients for the tissues of coniferous trees [55].

Corresponding columns of the stand-level matrix were then populated with summaries of the tree-level information from that stand, including stand age, SA (years); stand density, SD (trees $\mathrm{ha^{-1}}$); stand biomass growth (of survivors and recruits), SG (Mg C $\mathrm{ha^{-1}}$ $\mathrm{year^{-1}}$); stand biomass turnover due to litterfall, SLF (Mg C $\mathrm{ha^{-1}}$ $\mathrm{year^{-1}}$); stand biomass loss due to mortality, SM (Mg C $\mathrm{ha^{-1}}$ $\mathrm{year^{-1}}$); and stand biomass density, SB (Mg C $\mathrm{ha^{-1}}$). Stand net primary production, SNPP (Mg C $\mathrm{ha^{-1}}$ $\mathrm{year^{-1}}$), is defined as the difference between the photosynthetic fixation of carbon and autotrophic respiration of carbon, and was approximated from the sum of stand biomass growth and biomass turnover due to litterfall.

The subsequent description of forest biomass dynamics was based on the mean value of each variable across n stands of the simulated landscape. To facilitate a comparison with field observations, we reported predictions of net ecosystem biomass production (NEBP), defined as the net change in biomass for stands during time-intervals in which there were no stand-replacing disturbances:

$$\mathrm{NEBP} = \mathrm{SNPP} - \mathrm{SLF} - \mathrm{SM_{Sim,NSR}} - \mathrm{SM_{Pre,NSR}} \quad (7)$$

Net biome biomass disturbance (NBBD) was defined as the net change in biomass for stands during time-intervals where stand-replacing disturbances occurred:

$$\mathrm{NBBD} = \mathrm{SM_{Sim,SR}} - \mathrm{SM_{Pre,SR}} \quad (8)$$

Net biome biomass production (NBBP) was calculated as:

$$\text{NBBP} = \text{NEBP} - \text{BBD} \tag{9}$$

which is equal to net change in mean stand biomass density. Consistent with the differentiation between NEBP and NBBP, we also differentiated between the biomass residence time of intact ecosystems:

$$t_{\text{res},EB} = \frac{\text{SB}}{\text{SM}_{\text{Sim,NSR}} - \text{SM}_{\text{Pre,NSR}}} \tag{10}$$

and biomass residence time of the forest biome, including disturbances:

$$t_{\text{res},BB} = \frac{\text{SB}}{\text{SM}_{\text{Sim,NSR}} + \text{SM}_{\text{Pre,NSR}} + \text{SM}_{\text{Sim,SR}} - \text{SM}_{\text{Pre,SR}}} \tag{11}$$

2.3. Study Design and Analysis

Objectives of the study were achieved by conducting four analyses: (1) description of calibrated equations of recruitment, mortality, and growth; (2) description of single-stand predictions of biomass dynamics using the Sawtooth function driven with the calibrated equations; (3) description of the scaling relationship between changes in tree growth and landscape-scale forest biomass dynamics; and (4) sensitivity analysis of the scaling relationship between tree growth and stand biomass density. The procedures of each analysis are described in the following four sections.

2.3.1. Calibration of Equations

Equations describing the probability of recruitment and mortality were solved using the *fitglme* function, while equations for growth were solved using the *fitlme* function (MATLAB R2016a, The Mathworks Inc., Natick, MA, USA). A random effect was applied to the intercept at the level of field plots. To facilitate the interpretation of effects, all independent variables were standardized (i.e., centred by subtracting the mean and scaled by dividing the standard deviation) prior to fitting [57]. Coefficients, therefore, describe the change in the dependent variable caused by a +1 S.D. increase in each predictor variable. The performance of the growth models was based on the model efficiency coefficient (MEC). An MEC value of less than 0.00 indicates that the model is less skillful than simply applying the mean of observations, an MEC equal to 0.00 indicates that the model is equally as skillful as simply applying the mean, and MEC values of 1.00 explain 100 percent of the variation in observations. For the logistic regression models of recruitment and mortality, we used the area under the curve (AUC) statistic to describe model performance.

2.3.2. Behaviour of Single-Stand Simulations

To provide assurance that the Sawtooth function was functioning properly when driven with the Default 1 equations for each species, we summarized the general behaviour of single-stand simulations. Simulations were conducted for 500 years without imposing any stand-replacing disturbance to visualize the phases of initial regeneration and stand breakup that occur within a single stand. We additionally tested whether the model conformed to the expected dependence between average body size and stand density (i.e., the size-density relationship), or the 'Self-thinning Rule'. For a reference, we compared the simulated size-density relationship with a self-thinning function [24]. According to this implementation of the self-thinning rule, the thinning curve is defined by a parameter describing the average tree biomass that can be supported by a stand density of 1000 trees ha^{-1}, B_{ave1000}. To give Sawtooth simulations context, we included the expected dependence of stand density on average tree biomass by applying the self-thinning rule with B_{ave1000} set to 400 kg C tree^{-1}.

In all simulations, SD_{seed} was set to 200 trees ha^{-1}, $B_{\text{ag,seed,mu}}$ was set to 0.001 kg C, and $B_{\text{ag,seed,sig}}$ was set to 0.100 kg C. These values for SD_{seed}, $B_{\text{ag,seed,mu}}$, and $B_{\text{ag,seed,sig}}$ were parameterized to

reflect natural regeneration and model behaviour was largely uninfluenced by moderate variation in each value. Model behaviour was more strongly influenced by the parameterization of SD_{max}. Interestingly, an increase in SD_{max} increases the magnitude of gross biomass fluxes (e.g., net primary production, litterfall, and mortality), but has no effect on net ecosystem biomass production. Here, we set SD_{max} to 3500 trees ha^{-1}, which was safely above the peak values of predicted stand density reached in single-stand simulations, and which translated into estimates of stand net primary production within the range of expected values for boreal, cold-temperate, and maritime-temperate forests [58,59].

2.3.3. Scaling Relationships between Growth and Landscape-Scale Biomass Dynamics

To understand how changes in tree growth affected forest biomass dynamics, the Sawtooth function was run five times to analyze responses over a range of different perturbations in tree growth. Each simulation consisted of a hypothetical landscape of 1200 stands and was run for 3000 years. Adopting these dimensions prevented the stochasticity in simulations of mortality from significantly influencing results.

The perturbation in tree growth was *hardwired* into the code at the halfway point of each simulation (year 1500) by multiplying the prediction of tree growth from Equation (3) according to a stimulus factor, resulting in a step-change in tree growth between the first and second halves of the simulation. The effect of changes in tree growth on landscape-scale biomass dynamics was then assessed by calculating equilibrium responses for all stand-level variables output by the Sawtooth function. The equilibrium response was defined as the actual difference (or response ratio) between mean values of each variable during post-stimulus and pre-stimulus treatment periods. The pre-stimulus treatment period was defined from years 1000 to 1499 of the simulation, while the post-stimulus treatment period was defined from years 2501 to 3000 of the simulation, which safely allowed biomass dynamics to fully equilibrate following a change in boundary conditions. Two-sample *t*-tests were conducted to test for the significance of each response.

To understand whether scaling relationships varied with the magnitude of the growth stimulus, the growth stimulus factors were varied to include values of 0.5, 1.0, 2.0, 3.0, and 4.0 over the five simulations of each species. The 0.5 stimulus factor represents a 50% decrease in tree growth. The 1.0 stimulus factor acts as the reference level (no change in tree growth), while stimuli of 2.0, 3.0, and 4.0 describe 100%, 200%, and 300% increases in growth, respectively.

Following a convention commonly applied in economics and hydrology [60,61], we defined the *tree-growth elasticity* of stand biomass density as:

$$\varepsilon_{G,SB} = \frac{dSB/SB}{dG/G} \tag{12}$$

which describes the proportional change in stand biomass density divided by the proportional change in tree growth. A value of $\varepsilon_{G,SB} > 1$ implies a relatively elastic response of SB, implying the existence of positive system feedbacks. A value of $\varepsilon_{G,SB} < 1$ implies an inelastic response of SB, suggesting the presence of negative system feedbacks.

2.3.4. Sensitivity Analysis

To gain additional insight into the influence of model parameters on the scaling relationship, a sensitivity analysis was conducted to understand the influence of eight key model parameters. Whereas the previous five simulations of each species varied the growth stimulus, simulations for the sensitivity analysis implemented a constant growth stimulus factor to standardize results. For this purpose, a growth stimulus factor of 2.0 (a doubling in growth) was chosen as a standardized reporting benchmark. In each of the simulations, a different model parameter was modified by implementing a parameter adjustment factor of 1.25 (i.e., an 25% increase) while holding all other parameters constant.

3. Results

3.1. General Model Behaviour

As expected, coefficients of the Default 1 equations were consistently significant (Tables 2–4). The variance inflation factors were below 2.0 for all independent variables, indicating an absence of multicollinearity in the calibration samples. Models suggested that the mean annual probability of recruitment ranged from 0.72 and 1.92% year^{-1} depending on the species and depending on whether one referenced the conditional or marginal predictions (Table 2). In all species, recruitment rates decreased with an increasing stand-level aboveground biomass, as indicated by negative values of the a_1 coefficient. The AUC statistics for marginal predictions ranged from 0.72 to 0.75.

Table 2. Equations of annual probability of recruitment (P_r): Number of observations; number of unique plots; ratio between observations indicating recruitment and no recruitment; best estimates of the coefficients, a_0 and a_1, and standard errors (parentheses); mean of conditional and marginal predictions; area under the curve (AUC).

Statistic	Black Spruce	Interior Douglas-Fir	Western Hemlock
a_0	−4.470 (0.014)	−6.020 (0.024)	−5.463 (0.029)
a_1	−0.901 (0.009)	−0.991 (0.007)	−1.600 (0.014)
Mean predicted P_r (Cond.) (% year^{-1})	1.94	1.77	1.31
Mean predicted P_r (Marg.) (% year^{-1})	1.53	0.72	1.00
AUC (Cond.)	0.87	0.82	0.75
AUC (Marg.)	0.72	0.73	0.75

Mean annual probability of mortality ranged from 1.12% year^{-1} to 2.50% year^{-1} depending on the species and depending on whether one referenced the conditional or marginal predictions (Table 3). Interior Douglas-fir and western hemlock showed a U-shaped dependence of mortality on the aboveground biomass of trees, while black spruce showed the opposite pattern of size dependence, peaking at an intermediate size. It is worth noting that, contrary to expectation, the dependence of mortality on stand biomass density was negative in western hemlock. The AUC statistics for the marginal predictions ranged from 0.62 to 0.73.

Mean annual aboveground biomass growth (of individual trees) ranged from 0.50 to 3.88 kg C tree^{-1} yr^{-1} depending on the species and depending on whether one references the conditional or marginal predictions (Table 4). All species showed an initial positive dependence of growth on size, followed by a negative dependence on size, as indicated by positive and negative values of c_1 and c_2 coefficients, respectively. In all species, growth exhibited an inverse dependence on age, biomass of larger trees in the stand, and stand biomass density. The magnitude of the relationship between growth and stand biomass density was relatively weak in black spruce and interior Douglas-fir, while the relationship between growth and age was relatively weak in western hemlock.

Table 3. Equations of annual probability of mortality (P_m): Number of observations; number of unique plots; ratio of mortality and non-mortality observations; best estimates of the coefficients, $b_0 \ldots b_5$, and standard errors (parentheses); mean conditional and marginal predictions; area under the curve (AUC).

Statistic	Black Spruce	Interior Douglas-Fir	Western Hemlock
b_0	−4.556 (0.014)	−4.194 (0.021)	−4.846 (0.024)
b_1	0.090 (0.008)	−0.289 (0.010)	−0.068 (0.017)
b_2	−0.052 (0.009)	0.163 (0.006)	0.183 (0.010)
b_3	0.331 (0.012)	0.083 (0.011)	0.040 (0.013)
b_4	0.177 (0.012)	0.642 (0.008)	2.547 (0.019)
b_5	0.131 (0.015)	0.451 (0.010)	−2.217 (0.023)
Mean predicted P_m (Cond.) (% year^{-1})	1.12	1.70	1.89
Mean predicted P_m (Marg.) (% year^{-1})	1.17	2.50	1.38
AUC (Cond.)	0.82	0.81	0.83
AUC (Marg.)	0.68	0.62	0.73

Table 4. Species-specific models of annual tree growth, G_{ag} (kg C tree year^{-1}): Number of observations; number of unique plots; best estimates of the coefficients, $c_0 \ldots c_5$, and standard errors (parentheses); Mean of conditional and marginal predictions; model efficiency coefficient (MEC) for conditional and marginal predictions.

Statistic	Black Spruce	Interior Douglas-Fir	Western Hemlock
c_0	−0.839 (0.008)	0.343 (0.008)	0.529 (0.010)
c_1	0.492 (0.003)	1.092 (0.002)	1.556 (0.002)
c_2	−0.031 (0.002)	−0.198 (0.002)	−0.259 (0.001)
c_3	−0.127 (0.004)	−0.198 (0.005)	−0.030 (0.005)
c_4	−0.278 (0.003)	−0.487 (0.002)	−0.646 (0.003)
c_5	−0.060 (0.005)	−0.051 (0.004)	−0.135 (0.004)
Mean predicted G_{ag} (Cond.)	0.52	2.35	3.47
Mean predicted G_{ag} (Marg.)	0.50	2.41	3.88
MEC (Cond.)	0.60	0.80	0.80
MEC (Marg.)	0.23	0.61	0.65

Incorporating these equations for recruitment, mortality, and aboveground biomass growth into a stand-level model reproduced the expected patterns in the population of trees in a single stand (Figure 2). Following a stand-replacing disturbance, the stand biomass density was very low, translating into high recruitment (Figure 2a) and relatively low mortality (Figure 2b). Stand density reached a maximum value between 37 and 50 years after disturbance (Figure 2c). After an initial recovery phase, the stands reached a stem-exclusion phase [62]. Following a period of stand breakup, the stand biomass density reached a threshold in which recruitment started to exceed mortality again, leading to a second generation of trees. In general, population dynamics conform to the expected relationship between tree size and stand density, or the self-thinning rule (Figure 2d). However, it is worth noting that none of the species precisely followed a linear function in the log-log space of tree size and stand density, as exemplified by the self-thinning boundary when $B_{ave1000}$ was set to 400 kg C tree^{-1}. It is also worth noting how the predicted curves changed slightly between the first and second generations of the simulations.

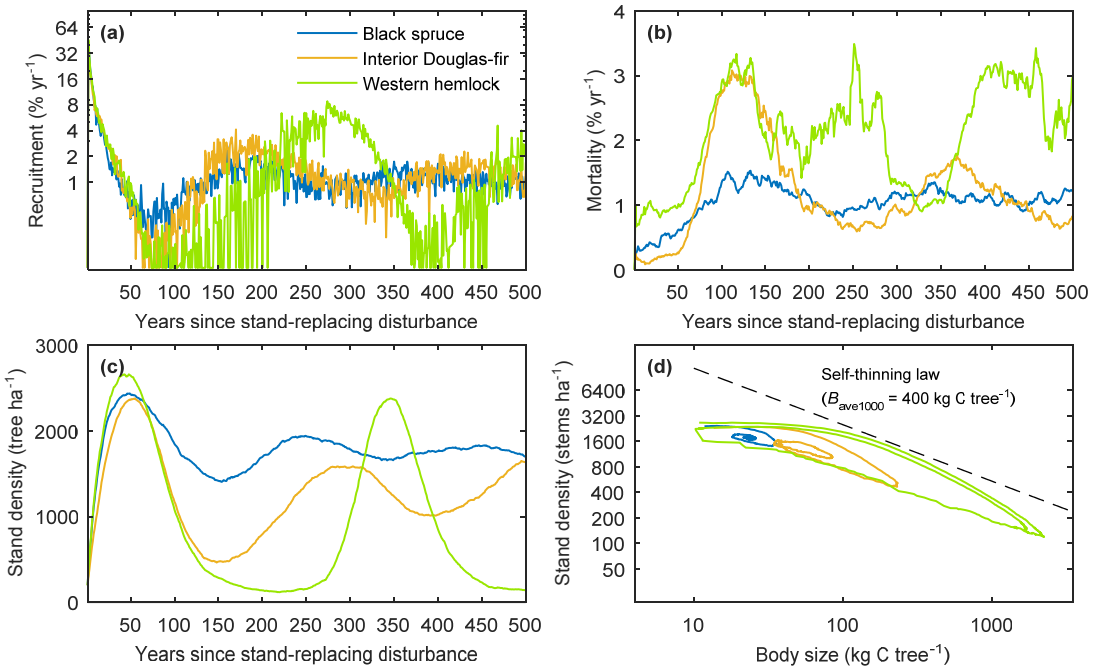

Figure 2. Single-stand population dynamics of black spruce, interior Douglas-fir, and western hemlock following natural regeneration from a stand-replacing disturbance: (**a**) annual probability of recruitment (note log scale of *y*-axis); (**b**) annual probability of mortality; (**c**) stand density; (**d**) size-density relationship (note log scales of *x*- and *y*-axis). yr, year.

During the regeneration phase, net primary production increased from zero to peak values between 50 and 100 years after disturbance (Figure 3a), while biomass losses due to litterfall and mortality started off at zero and reached peak values between 100 and 150 years after disturbance (Figure 3b). During initial regeneration, trees acted as a net biomass sink, as indicated by positive values of NEBP (Figure 3c). At times after disturbance, ranging from 105 to 145 years, the average annual NEBP transitioned from positive to negative, as biomass losses due to mortality started to exceed biomass growth. Although the pattern was extremely muted by the overall low values of biomass in black spruce, all species showed a pronounced decrease in stand biomass density during a phase of stand break-up before reaching threshold levels of low stand biomass density that triggered population growth (Figure 3d).

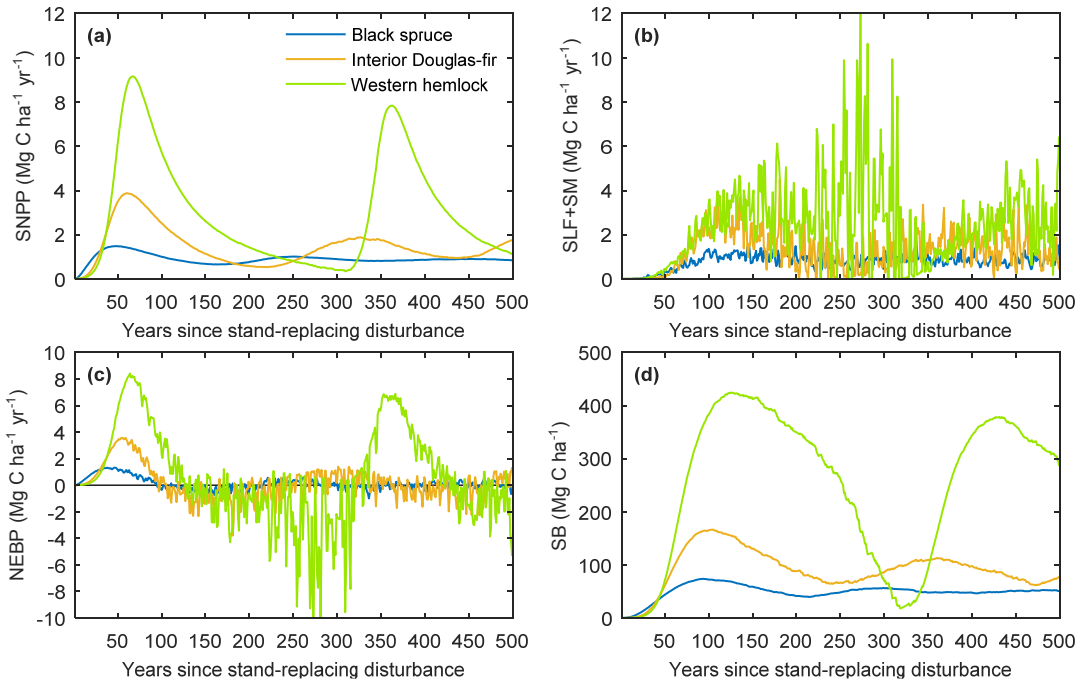

Figure 3. Single-stand biomass dynamics of black spruce, interior Douglas-fir, and western hemlock following natural regeneration from a stand-replacing disturbance: (**a**) stand-level net primary production (SNPP); (**b**) stand-level biomass turnover due to litterfall plus mortality (SLF + SM); (**c**) net ecosystem biomass production (NEBP); (**d**) stand-level biomass density (SB). yr, year.

3.2. Equilibrium Responses to a Change in Tree Growth

Whereas Figures 2 and 3 illustrated the general behaviour of the models from a single stand simulation, the experimental simulations of the study were conducted for a landscape of 1200 stands, as exemplified by the simulations of western hemlock in Figure 4. Extending the simulations over 3000 years allowed the pre-stimulus and post-stimulus treatment periods to safely avoid abnormal variability of the initial regeneration following start-up from years 0 to ~500, and again following the perturbation at year 1500 (Figure 4).

Scatterplots pairing each response ratio with each magnitude of tree growth stimulus never showed perfect 1:1 relationships (Figure 5). That is, regardless of the variable in question, the magnitude of relative response to varying perturbations in individual-tree growth was not linearly related to the magnitude of the growth stimulus factor. The only instances where the relationship came close to a 1:1 relationship was for the mean tree growth of black spruce and interior Douglas-fir (Figure 5a). It is counterintuitive *prima facie* that the response in landscape-average tree growth did not scale perfectly with the imposed growth stimulus factor. This decoupling demonstrates the dynamic nature of the models. For example, if the stimulus factor that is applied to growth consistently increases the size of the tree and growth eventually decreases with size, then the perturbation in growth will become less influential (Equation (3)). The magnitude of decoupling appeared to be minor for black spruce and interior Douglas-fir, but substantial for western hemlock. For example, imposing a 300% perturbation in tree growth only translated into a 168% increase in landscape-scale tree growth of western hemlock.

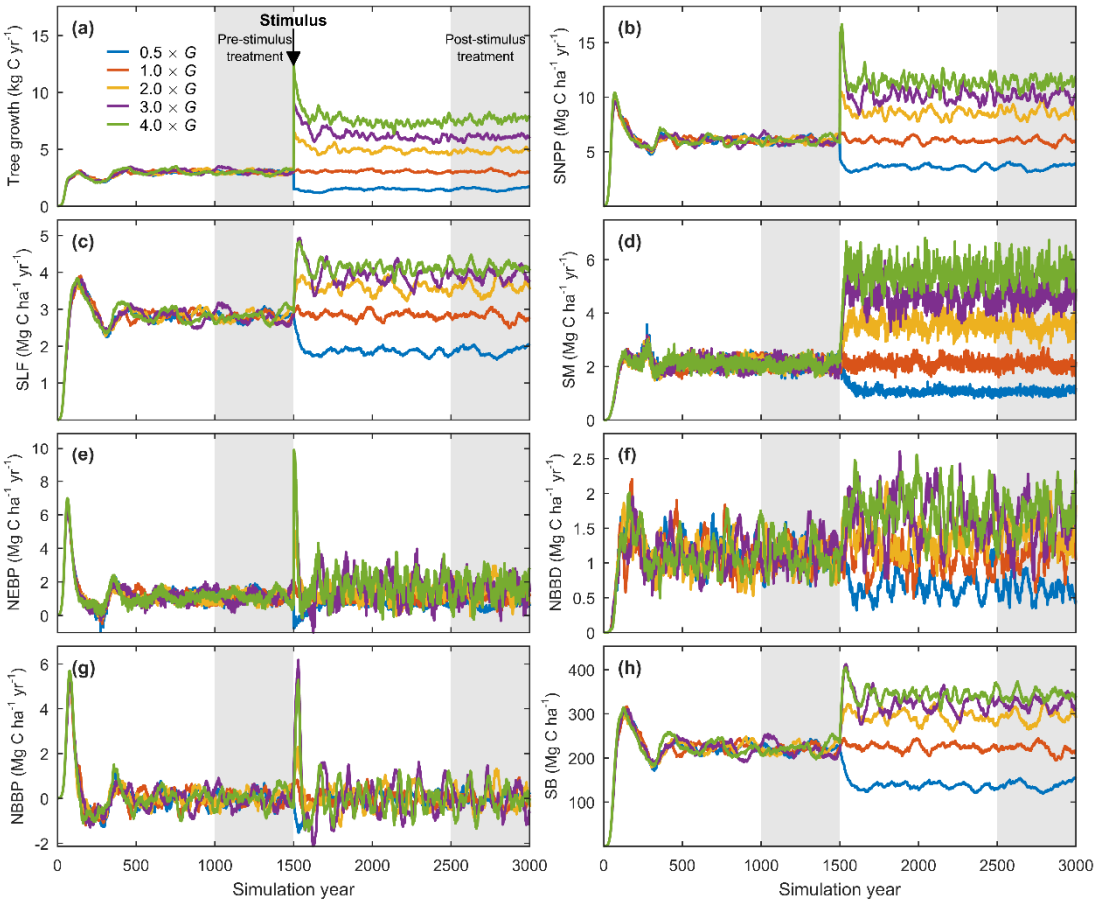

Figure 4. Biomass dynamics of a western hemlock landscape subject to a perturbation in tree growth at the halfway point of the simulations, ranging from stimulus factors of 0.5 (a 50% decrease) to 4.0 (a 300% increase): (**a**) mean tree growth; (**b**) mean net primary production; (**c**) mean litterfall; (**d**) mean mortality; (**e**) mean net ecosystem biomass production; (**f**) mean net biome biomass disturbance; (**g**) mean net biome biomass production; (**h**) mean stand biomass density. yr, year.

Positive stimulation of tree growth translated into decreases in landscape-average tree age and stand density (Figure 5b,c) and increases in mean stand-level net primary production (Figure 5d), litterfall (Figure 5e), mortality (Figure 5f), net ecosystem biomass production (Figure 5g), net biome biomass disturbance (Figure 5h), and biomass density (Figure 5i). Even though landscape-average tree growth was the least responsive to the growth stimulus factor in western hemlock, the relative response of stand-level net primary production was the greatest in western hemlock, implying a high degree of complexity in responses (Figure 5d).

Conversely, a negative stimulation of tree growth translated into increases in mean tree age and stand density, and decreases in stand-level net primary production, litterfall, mortality, net ecosystem biomass production, net biome biomass production, and stand biomass density (Figure 5).

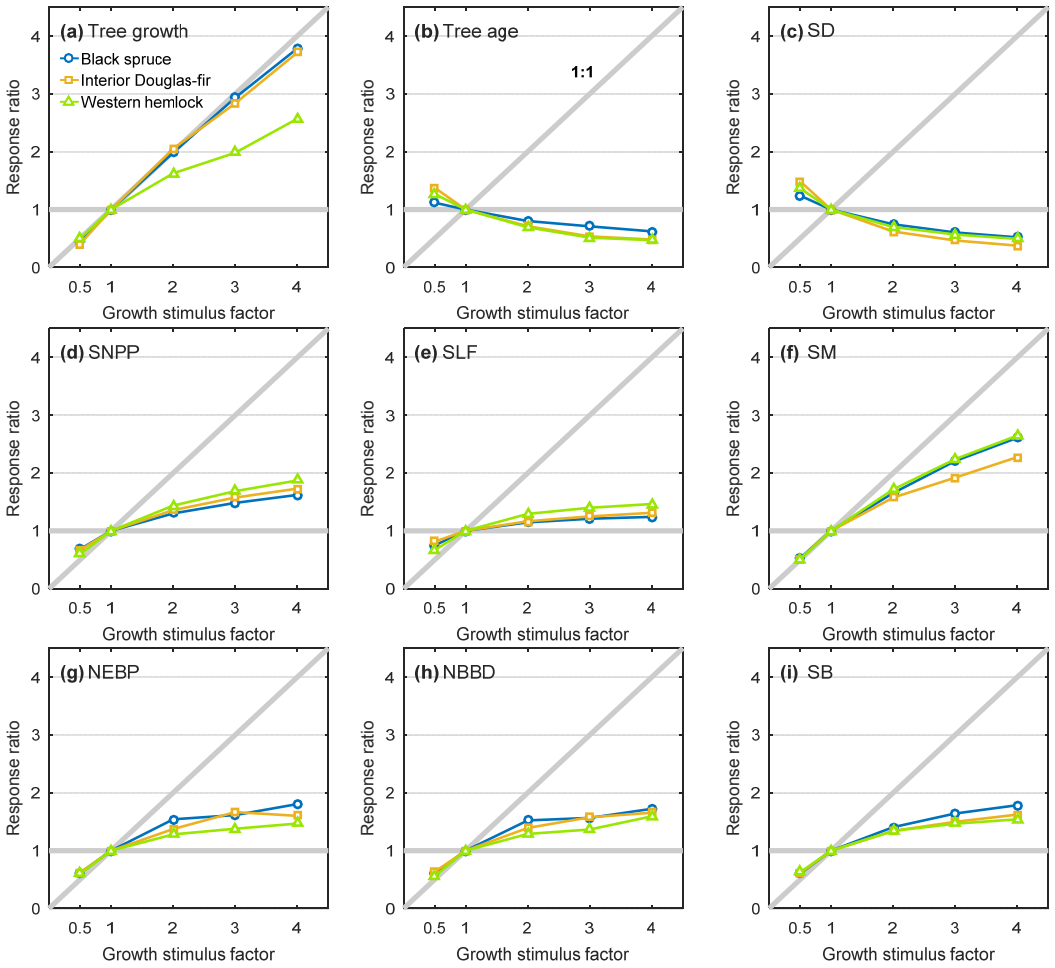

Figure 5. Equilibrium response to varying perturbations in tree growth expressed as the mean value during the post-stimulus treatment period divided by the mean value during the pre-stimulus treatment period. Perturbations ranged from stimulus factors of 0.5 (50% decrease in growth), 1 (no change in growth), 2 (100% increase), 3 (200% increase), and 4 (300% increase). SD: Stand density; SNPP: Stand net primary production; SLF: Stand litterfall; SM: Stand mortality; NEBP: Net ecosystem biomass production; NBBD: Net biome biomass disturbance; SB: Stand biomass.

On average, imposing a tree growth stimulus of 2 (a doubling) only translated into a 37% increase in net primary production, while litterfall and mortality increased by 20% and 65%, respectively (Table 5). The mean 36% response of stand biomass density was similar to that of net primary production, but there was no coherence between responses of net primary production and stand biomass density among species. On average, stand density decreased by 31%, while biome-scale biomass residence time decreased by 13%. The tree-growth elasticity of stand biomass density ranged from 0.33 for interior Douglas-fir to 0.55 for western hemlock. There was no coherence between the response ratio of stand biomass density and tree-growth elasticity among species.

A close-up look at the response of each species to the doubling in tree growth illustrated the transient nature of the response of net ecosystem biomass production (Figure 6). Much like the first regeneration cycle of any model simulation, the uniform change in growth rates across entire landscapes triggered low-frequency dynamics that dissipated over centuries, although they appeared highly muted in the less-productive black spruce simulations. In general, the stimulus was followed by phases of aggradation, transition, and finally steady state [63]. The responses closely resembled a general class of "growth with limited overshoot followed by stabilization" [64]. Although the broad perspective given by Figure 6 made the transition phase look weak, it is easy to see how the unique

high magnitude and transient nature of stand biomass densities achieved during the first aggradation and transition sequence could have important impacts on the forest sector. The positive response of net ecosystem biomass production terminates at years ranging from 50 to 95 years after the perturbation in interior Douglas-fir and western hemlock, respectively.

Table 5. Equilibrium responses to a doubling in the growth rate of individual trees for black spruce, interior Douglas-fir, and western hemlock: Δ indicates the difference (post-stimulus mean—pre-stimulus mean); response ratio (post-stimulus mean/pre-stimulus mean); tree-growth elasticity, $\varepsilon_{G,X} = (\Delta G/G)/(\Delta X/X)$, where X is the independent variable of interest; (p-values indicate the probability that the difference between treatments arises from chance according to two-sample t-tests.

Statistic	Pre-Stim. Mean	Post-Stim. Mean	Δ	Response Ratio	$\varepsilon_{G,X}$	p-Value
Tree growth (kg C tree^{-1} year^{-1})						
Black spruce	0.36	0.72	0.35	1.98	N.A.	<0.001
Interior Douglas-fir	0.79	1.61	0.83	2.05	N.A.	<0.001
Western hemlock	2.99	4.86	1.87	1.63	N.A.	<0.001
Mean	1.38	2.40	1.02	1.89	N.A.	<0.001
Stand net primary production (Mg C ha^{-1} year^{-1})						
Black spruce	2.87	3.74	0.87	1.30	0.31	<0.001
Interior Douglas-fir	2.94	4.00	1.05	1.36	0.34	<0.001
Western hemlock	6.01	8.63	2.62	1.44	0.70	<0.001
Mean	3.94	5.45	1.51	1.37	0.45	<0.001
Stand litterfall (Mg C ha^{-1} year^{-1})						
Black spruce	1.95	2.24	0.29	1.15	0.15	<0.001
Interior Douglas-fir	1.35	1.57	0.22	1.16	0.16	<0.001
Western hemlock	2.78	3.60	0.82	1.29	0.47	<0.001
Mean	2.03	2.47	0.44	1.20	0.26	<0.001
Stand mortality (Mg C ha^{-1} year^{-1})						
Black spruce	0.71	1.18	0.47	1.65	0.66	<0.001
Interior Douglas-fir	1.16	1.82	0.67	1.58	0.55	<0.001
Western hemlock	2.06	3.55	1.48	1.72	1.15	<0.001
Mean	1.31	2.18	0.87	1.65	0.79	<0.001
Stand biomass density (Mg C ha^{-1})						
Black spruce	47	66	19	1.41	0.41	<0.001
Interior Douglas-fir	88	118	30	1.34	0.33	<0.001
Western hemlock	219	294	75	1.34	0.55	<0.001
Mean	118	159	41	1.36	0.43	<0.001
Stand density (tree ha^{-1})						
Black spruce	1802	1338	−463	0.74	−0.26	<0.001
Interior Douglas-fir	1301	806	−495	0.62	−0.36	<0.001
Western hemlock	1168	815	−353	0.70	−0.48	<0.001
Mean	1424	986	−437	0.69	−0.37	<0.001
Residence time, ecosystem (years)						
Black spruce	65.5	55.7	−9.8	0.85	−0.15	<0.001
Interior Douglas-fir	75.9	64.6	−11.3	0.85	−0.14	<0.001
Western hemlock	106.1	82.9	−23.2	0.78	−0.35	<0.001
Mean	82.5	67.7	−14.7	0.83	−0.21	<0.001
Residence time, biome (years)						
Black spruce	50.2	43.5	−6.7	0.87	−0.14	<0.001
Interior Douglas-fir	55.3	48.6	-6.7	0.88	−0.11	<0.001
Western hemlock	68.5	58.7	−9.8	0.86	−0.23	<0.001
Mean	58.0	50.3	−7.7	0.87	−0.16	<0.001

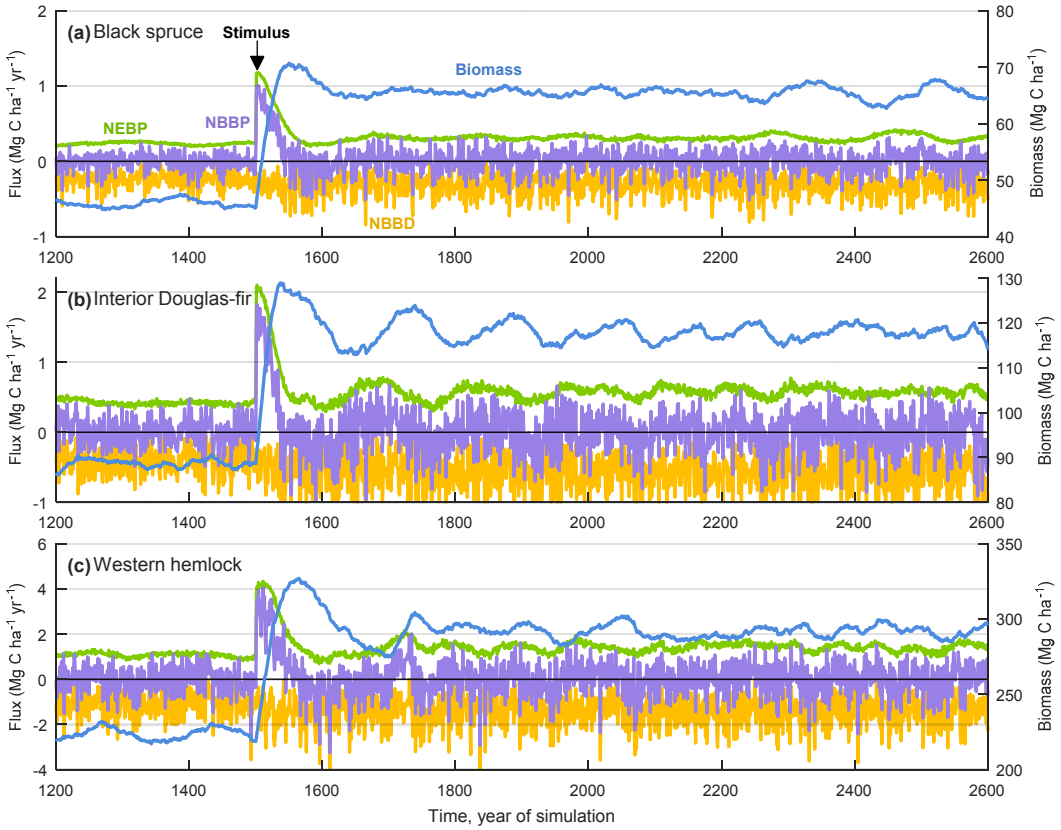

Figure 6. Landscape-mean biomass fluxes (left axis) and stand biomass density (right axis) for: (**a**) black spruce; (**b**) interior Douglas-fir; and (**c**) western hemlock. yr, year.

As the scaling relationships depended strongly on the magnitude of tree growth stimulus factor (Figure 5), the results in Table 5 and Figure 6 are specific to, and only representative of, the responses to a doubling above contemporary rates of tree growth (i.e., above the rates that are predicted based on calibration against recent field observations). For retrospective analyses, such as reconstructions of historical tree growth from tree-ring chronologies, it is likely more meaningful to shift the perspective by assessing the scaling relationships for a hypothetical increase in growth from some reduced starting rate (e.g., an estimate of pre-industrial growth rates) up to contemporary rates. Here, we again rely on a hypothetical doubling from a lower baseline rate of growth as a reporting benchmark (Table 6). Despite similar decreases in stand density and biomass residence time, a retrospective doubling tree growth stimulus scenario indicated a mean tree-growth elasticity of stand biomass density, $\varepsilon_{G,SB}$ = 0.72 (Table 6), that was substantially greater than that reported for a doubling above contemporary rates of growth (Table 5).

Table 6. Equilibrium responses to a hypothetical retrospective growth enhancement scenario: an increase in tree growth from 50% below contemporary rates to contemporary rates, where contemporary rates are defined by the baseline simulation (i.e., representative of the calibrations against recent field plot observations). See Table 5 for additional details.

Statistic	50% Below Contemporary	Contemporary	Δ	Response Ratio	$\varepsilon_{G,X}$	*p*-Value
Tree growth (kg C tree^{-1} year^{-1})						
Black spruce	0.17	0.36	0.19	2.17	N.A.	<0.001
Interior Douglas-fir	0.32	0.79	0.47	2.47	N.A.	<0.001
Western hemlock	1.51	3.01	1.51	2.00	N.A.	<0.001
Mean	0.66	1.39	0.72	2.21	N.A.	<0.001
Stand net primary production (Mg C ha^{-1} year^{-1})						
Black spruce	1.96	2.86	0.91	1.46	0.59	<0.001
Interior Douglas-fir	1.96	2.95	0.99	1.50	0.56	<0.001
Western hemlock	3.60	6.01	2.41	1.67	0.80	<0.001
Mean	2.51	3.94	1.43	1.54	0.65	<0.001
Stand litterfall (Mg C ha^{-1} year^{-1})						
Black spruce	1.45	1.94	0.49	1.34	0.47	<0.001
Interior Douglas-fir	1.10	1.36	0.25	1.23	0.31	<0.001
Western hemlock	1.87	2.80	0.93	1.50	0.67	<0.001
Mean	1.47	2.03	0.56	1.35	0.48	<0.001
Stand mortality (Mg C ha^{-1} year^{-1})						
Black spruce	0.36	0.69	0.33	1.91	0.88	<0.001
Interior Douglas-fir	0.60	1.17	0.57	1.96	0.82	<0.001
Western hemlock	1.06	2.08	1.02	1.96	0.98	<0.001
Mean	0.67	1.31	0.64	1.94	0.89	<0.001
Stand biomass density (Mg C ha^{-1})						
Black spruce	28	46	18	1.66	0.74	<0.001
Interior Douglas-fir	54	88	35	1.64	0.66	<0.001
Western hemlock	138	221	83	1.60	0.75	<0.001
Mean	73	118	45	1.64	0.72	<0.001
Stand density (tree ha^{-1})						
Black spruce	2246	1810	−436	0.81	−0.45	<0.001
Interior Douglas-fir	1933	1297	−636	0.67	−0.82	<0.001
Western hemlock	1582	1158	−424	0.73	−0.73	<0.001
Mean	1920	1422	−499	0.74	−0.67	<0.001
Residence time, ecosystem (years)						
Black spruce	76.2	66.3	−9.9	0.87	−0.11	<0.001
Interior Douglas-fir	90.1	75.7	−14.4	0.84	−0.11	<0.001
Western hemlock	129.9	106.0	−23.9	0.82	−0.18	<0.001
Mean	98.7	82.7	−16.1	0.84	−0.13	<0.001
Residence time, biome (years)						
Black spruce	54.5	49.2	−5.3	0.90	−0.08	<0.001
Interior Douglas-fir	62.4	55.7	−6.7	0.89	−0.07	<0.001
Western hemlock	81.7	68.8	−12.9	0.84	−0.16	<0.001
Mean	66.2	57.9	−8.3	0.88	−0.10	<0.001

3.3. Sensitivity Analysis

All tested model parameters contributed to the magnitude of the decoupling of stand biomass from perturbations in tree growth according to sensitivity analysis (Figure 7). In black spruce, increasing the return-interval of stand-replacing fire by 25% led to a decrease in the positive response of stand biomass from the actual response of 41% (Table 5) to 40% ($\Delta SB = -0.009$ in Figure 7a). Similar sensitivities were expressed by interior Douglas-fir (Figure 7b) and western hemlock (Figure 7c). A 25% intensification in the negative dependence of recruitment on stand biomass (a_1 in Table 2) similarly decreased the response of stand biomass in all species. Likewise, a 25% intensification in the positive dependence of mortality on the biomass of larger trees (b_4 in Table 3), or the negative dependence of growth on

the biomass of larger trees (c_4 in in Table 3), consistently decreased the response of stand biomass. The additional consideration of an absolute measure of stand competition on mortality was almost as influential, although we acknowledge the counter-intuitive direction of the relationship for western hemlock mortality, which translated into an increase in the forest biomass response to growth enhancement (Figure 7c). Increasing biomass turnover rates by 25% consistently led to decreases in the forest biomass response to growth enhancement in all species, with a slightly greater influence of foliage and fine-root turnover parameters.

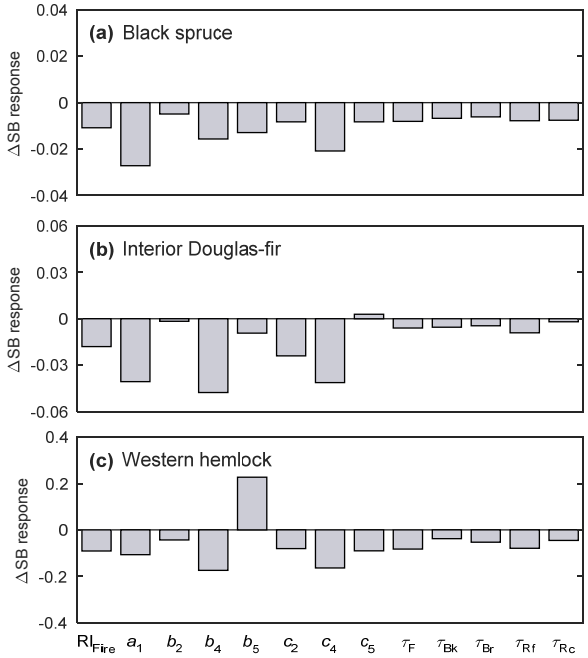

Figure 7. Sensitivity analysis: The effect of a 25% increase in parameters on the response of stand biomass (SB) to a doubling of tree growth rate. Tested parameters include: Return-interval of stand-replacing fire (RI_{Fire}), dependence of recruitment rate on stand biomass (a_1), dependence of mortality rate on the square of tree biomass (b_2), biomass of larger trees in the stand (b_4) and stand biomass (b_5), dependence of aboveground biomass growth rate on tree biomass (c_2), biomass of larger trees in the stand (c_4) and stand biomass (c_5), and turnover rates for foliage, branches, bark, fine roots, and coarse roots (τ_F, τ_{Br}, τ_{Bk}, τ_{Rf}, τ_{Rc}).

4. Discussion and Conclusions

Understanding how changes in tree growth translate into stand biomass density is important for predicting how patterns of growth enhancement and growth decline will affect forest biomes. By analyzing relationships between growth and longevity for several species, Bugmann and Bigler [19] argued that any growth enhancement caused by carbon dioxide fertilization would lead to disproportionately small increases in stand biomass density, even without any change in the longevity of trees, but that such growth enhancement would likely cause a decrease in the longevity trees, and that landscape-scale responses would, therefore, be close to zero. By exploring results from an individual-based Growth and Yield model for three additional species, our study adds to quantitative constraints on the scaling relationship between tree growth and landscape-scale biomass dynamics, including stand biomass density.

Consistent with Bugmann and Bigler [19], we hypothesized that the dependence of recruitment, mortality, and growth on tree size and stand competition would act to decouple changes in forest biomass density from changes in tree growth (Hypothesis 1). A hypothetical future growth enhancement scenario, simulated by introducing a doubling in the growth rate of trees above contemporary rates, only translated into relative changes in stand biomass density ranging from 34% to 41%.

This corresponded with the tree-growth elasticity of stand biomass density ranging from 0.33 to 0.55. Predictions from this type of model, therefore, supported Hypothesis 1. Sensitivity analysis clearly demonstrated that stand competition was a primary contributor to negative feedbacks; not only did stand competition affect all three rates (recruitment, mortality, and growth), but the magnitude of the effects on tree growth elasticity of stand biomass density were also relatively strong. Stand density decreased by 31%, which was comparable to decreases identified in response to 100 years of growth enhancement identified at field plots in temperate forests in Europe [11]. Sensitivity analysis also demonstrated that the ontogeny of trees, the disturbance regime (i.e., magnitude of disturbance return-interval), and the magnitude of biomass turnover rates also contributed to the decoupling of stand biomass density from tree growth. Collectively, these processes meant that a doubling in tree growth caused decreases in biomass residence time and a disproportionately greater response of mortality (65%) than of net primary production (37%).

Our results are, therefore, consistent with the first two conclusions from Bugmann and Bigler [19]; stand biomass density was strongly decoupled from growth enhancement and this partially reflected a decrease in the longevity of trees, as evidenced by decreases in biomass residence time and mean tree age. However, whereas Bugmann and Bigler [19] concluded that the negative feedbacks were strong enough to preclude significant responses of stand biomass density arising from a growth stimulus of 30%, we found that a growth stimulus of 30% would translate into a 9% increase in stand biomass density (Figure 5i).

Evidence suggesting that effects of growth enhancement on landscape-scale forest biomass density are not completely precluded by system feedbacks has implications for the interpretation of studies that identify long-term trends in the growth rate of individual trees, or the interpretation of studies that report experimental responses of individual-tree growth to global change factors. For example, compiling experiments that expose seedlings or field-grown trees to carbon dioxide enrichment indicate mean relative increases in biomass growth of 41% and 61%, respectively, between those grown at an ambient carbon dioxide concentration (a mean value of 350 ppm) vs. an enriched carbon dioxide concentration (a mean value of 714 ppm) [15,65]. Combining the two datasets indicates a mean 44% increase in biomass growth. Although there are many other factors to consider, we propose based on the behaviour of our tested species (Figure 5i), it is likely that the above carbon-dioxide response of tree growth translates into an increase of 17% in stand-level biomass density. Similar exercises would apply to other potential global change factors.

The results also have implications for the interpretation of studies that identify long-term-trends in tree mortality. Although periodic droughts, warming, and the increasing evaporative demand of the atmosphere are clearly implicated in many reports of increasing tree mortality [26,66–68], considerable uncertainty exists in the magnitude of interactions between external hydrological conditions and competition and between external hydrological conditions, tree size, and age [26,32,69–73]. If one assumes that global change factors have increased tree growth, then a proportion of recent evidence indicating increasing time trends in tree mortality may reflect negative feedback responses to growth enhancement. Where interactions between size, competition, and external hydrological conditions are significant, water stress may be the inciting factor (proximate cause), while the gradual acceleration of ontogeny and intensified competition may be the predisposing risk (ultimate cause) for long-term positive trends in tree mortality.

We also hypothesized that the scaling relationship between changes in tree growth and stand biomass density would be independent of the magnitude of the tree growth stimulus (Hypothesis 2). This hypothesis was not supported. In all species, there was a distinct saturation in the response of stand biomass density as the stimulus of tree growth increased from 0% to 300%. In the context of global change factors, we can, therefore, expect differences in the scaling relationship between the past and future.

Lastly, we hypothesized that, across species, the degree of decoupling would increase with initial forest biomass density (Hypothesis 3), which was not clearly supported. Whereas the response ratio

of forest biomass density was greatest for black spruce, the tree-growth elasticity of forest biomass density was the greatest in western hemlock (Table 5). Hence, the research question was stymied by ambiguity in which metric best describes the scaling relationship. In addition to discrepancies between the species ranking of response ratios and tree-growth elasticities, the overall range of values was also relatively narrow. For example, in the retrospective growth enhancement scenario (Table 6), the response ratio of stand biomass density only ranged from 0.60 to 0.66. Further testing of other species is therefore required to further understand how universal these scaling relationships are across a diverse range of forests.

Limitations in the analysis and model applied here raise several caveats and open questions. With respect to the analysis, the results only focused on how changes in tree growth resonate through an otherwise stationary system; everything else, including recruitment, background mortality, and disturbance, were held constant. While this allowed us to isolate the effect of tree growth, it ignored environmental changes that are simultaneously influencing biomass-dense forests through changes in the rates of tree mortality [8,54,74,75]. As the simulations consisted of single-species stands, potential effects of tree growth stimulation on rates of succession were also not considered. The independence of biomass turnover rates (litterfall) on tree size and independence with the environmental change may influence these results. By considering three tree species of varying climate and overall growth potential, we showed that there are non-trivial differences among species in the scaling between tree growth and landscape-scale forest biomass. That said, we have treated the field samples as a single representative sample despite covering broad geographic and environmental distributions. Hence, we might expect these results to be generalizations of the species behaviour and inapplicable to any specific stand of the species. Lastly, the study identifies that any substantial enhancement in the growth of trees will translate into large increases in litterfall and mortality. Additional studies are therefore required to understand what the inelastic nature of stand biomass density means for net ecosystem carbon balance by simulating the fate of carbon entering dead organic matter.

By referencing a relatively simple individual-based Growth and Yield model, these results are strongly dependent on an empirical representation of ontogeny and resource competition, which likely has strengths and weaknesses. It is therefore important to consider evidence from a range of modelling approaches, including those that are more mechanistic and comprehensive, and using consistent reference levels to further constrain how global change factors affect forest biomass dynamics.

Acknowledgments: This research was supported by the Pacific Institute for Climate Solutions. We thank the work force involved in the collection of field plot data, including the British Columbia Ministry of Forests, Lands and Natural Resource Operations and Rural Development, Alberta Sustainable Resource Development, Saskatchewan Ministry of Environment Forest Service, Manitoba Conservation Forestry Branch, Ontario Ministry of Natural Resources, Nova Scotia Department of Natural Resources, New Brunswick Natural Resources, Newfoundland and Labrador Environment and Conservation, and the USDA Forest Service Forest Inventory and Analysis.

Author Contributions: R.A.H. designed the study and performed the simulations. R.A.H. and W.A.K. analyzed the results and wrote the article.

Conflicts of Interest: The authors declare no conflicts of interest.

References

1. Galbraith, D.; Malhi, Y.; Affum-Baffoe, K.; Castanho, A.D.A.; Doughty, C.E.; Fisher, R.A.; Lewis, S.L.; Peh, K.S.-H.; Phillips, O.L.; Quesada, C.A.; et al. Residence times of woody biomass in tropical forests. *Plant Ecol. Divers.* **2013**, *6*, 139–157. [CrossRef]
2. Zhang, L.; Luo, Y.; Yu, G.; Zhang, L. Estimated carbon residence times in three forest ecosystems of eastern China: Applications of probabilistic inversion. *J. Geophys. Res. Biogeosci.* **2010**, *115*. [CrossRef]
3. Zhou, X.; Zhou, T.; Luo, Y. Uncertainties in carbon residence time and NPP-driven carbon uptake in terrestrial ecosystems of the conterminous USA: A Bayesian approach. *Tellus B Chem. Phys. Meteorol.* **2012**, *64*, 17223. [CrossRef]

4. Ciais, P.; Sabine, C.; Bala, G.; Bopp, L.; Brovkin, V. Carbon and Other Biogeochemical Cycles. In *Climate Change 2013: The Physical Basis*; Contribution of Working Group I to the Fifth Assessment Report of the Intergovernmental Panel on Climate Change; Cambridge University Press: New York, NY, USA, 2013.
5. King, A.; Dilling, L.; Zimmerman, G.; Fairman, D.; Houghton, R.; Marland, G.; Rose, A.; Wilbanks, T. *The First State of the Carbon Cycle Report (SOCCR)*; U.S. Climate Change Science program Synthesis and Assessment product 2.2; 2007. Available online: http://cdiac.ess-dive.lbl.gov/SOCCR/pdf/sap2-2-final-all.pdf (accessed on 5 January 2018).
6. Prentice, I.; Farquhar, G.; Fasham, M.; Goulden, M.; Heimann, M.; Jaramillo, V.; Kheshgi, H.; Le Quere, C.; Scholes, R.; Wallace, D. The Carbon Cycle and Atmospheric Carbon Dioxide. In *Climate Change 2001: The Physical Science Basis*; Contribution of Working Group I to the Fourth Assessment Report of the Intergovernmental Panel on Climate Change; Cambridge University Press: New York, NY, USA, 2001.
7. Fang, J.; Kato, T.; Guo, Z.; Yang, Y.; Hu, H.; Shen, H.; Zhao, X.; Kishimoto-Mo, A.W.; Tang, Y.; Houghton, R.A. Evidence for environmentally enhanced forest growth. *Proc. Natl. Acad. Sci. USA* **2014**, *111*, 9527–9532. [CrossRef] [PubMed]
8. Hember, R.A.; Kurz, W.A.; Coops, N.C. Increasing net ecosystem biomass production of Canada's boreal and temperate forests despite decline in dry climates. *Glob. Biogeochem. Cycles* **2017**, *31*, 134–158. [CrossRef]
9. Kauppi, P.E.; Posch, M.; Pirinen, P. Large impacts of climatic warming on growth of boreal forests since 1960. *PLoS ONE* **2014**, *9*, e111340. [CrossRef] [PubMed]
10. Pan, Y.; Birdsey, R.A.; Fang, J.; Houghton, R.; Kauppi, P.E.; Kurz, W.A.; Phillips, O.L.; Shvidenko, A.; Lewis, S.L.; Canadell, J.G.; et al. A large and persistent carbon sink in the world's forests. *Science* **2011**, *333*, 988–993. [CrossRef] [PubMed]
11. Pretzsch, H.; Biber, P.; Schütze, G.; Uhl, E.; Rötzer, T. Forest stand growth dynamics in Central Europe have accelerated since 1870. *Nat. Commun.* **2014**, *5*, 4967. [CrossRef] [PubMed]
12. Drake, B.G.; Gonzàlez-Meler, M.A.; Long, S.P. More efficient plants: A consequence of rising atmospheric CO_2? *Annu. Rev. Plant Biol.* **1997**, *48*, 609–639. [CrossRef] [PubMed]
13. Idso, K.E.; Idso, S.B. Plant responses to atmospheric CO_2 enrichment in the face of environmental constraints: A review of the past 10 years' research. *Agric. For. Meteorol.* **1994**, *69*, 153–203. [CrossRef]
14. LeBauer, D.S.; Treseder, K.K. Nitrogen limitation of net primary productivity in terrestrial ecosystems is globally distributed. *Ecology* **2008**, *89*, 371–379. [CrossRef] [PubMed]
15. Norby, R.; Wullschleger, S.; Gunderson, C.; Johnson, D.; Ceulemans, R. Tree responses to rising CO_2 in field experiments: Implications for the future forest. *Plant Cell Environ.* **1999**, *22*, 683–714. [CrossRef]
16. Saxe, H.; Ellsworth, D.S.; Heath, J. Tree and forest functioning in an enriched CO_2 atmosphere. *New Phytol.* **1998**, *139*, 395–436. [CrossRef]
17. Way, D.A.; Oren, R. Differential responses to changes in growth temperature between trees from different functional groups and biomes: A review and synthesis of data. *Tree Physiol.* **2010**, *30*, 669–688. [CrossRef] [PubMed]
18. Xia, J.; Wan, S. Global response patterns of terrestrial plant species to nitrogen addition. *New Phytol.* **2008**, *179*, 428–439. [CrossRef] [PubMed]
19. Bugmann, H.; Bigler, C. Will the CO_2 fertilization effect in forests be offset by reduced tree longevity? *Oecologia* **2011**, *165*, 533–544. [CrossRef] [PubMed]
20. Friend, A.D.; Lucht, W.; Rademacher, T.T.; Keribin, R.; Betts, R.; Cadule, P.; Ciais, P.; Clark, D.B.; Dankers, R.; Falloon, P.D.; et al. Carbon residence time dominates uncertainty in terrestrial vegetation responses to future climate and atmospheric CO_2. *Proc. Natl. Acad. Sci. USA* **2014**, *111*, 3280–3285. [CrossRef] [PubMed]
21. Manusch, C.; Bugmann, H.; Heiri, C.; Wolf, A. Tree mortality in dynamic vegetation models—A key feature for accurately simulating forest properties. *Ecol. Model.* **2012**, *243*, 101–111. [CrossRef]
22. Körner, C. Plant CO_2 responses: An issue of definition, time and resource supply. *New Phytol.* **2006**, *172*, 393–411. [CrossRef] [PubMed]
23. Westoby, M. The Self-Thinning Rule. In *Advances in Ecological Research*; MacFadyen, A., Ford, E.D., Eds.; Academic Press: London, UK, 1984; pp. 167–225.
24. Landsberg, J.; Sands, P. *Physiological Ecology of Forest Production: Principles, Processes and Models*, 1st ed.; Elsevier Inc.: Boston, MA, USA, 2011.

25. Caspersen, J.P.; Vanderwel, M.C.; Cole, W.G.; Purves, D.W. How stand productivity results from size- and competition-dependent growth and mortality. *PLoS ONE* **2011**, *6*, e28660. [CrossRef] [PubMed]
26. Hember, R.A.; Kurz, W.A.; Coops, N.C. Relationships between individual-tree mortality and water-balance variables indicate positive trends in water stress-induced tree mortality across North America. *Glob. Chang. Biol.* **2017**, *23*, 1691–1710. [CrossRef] [PubMed]
27. Holzwarth, F.; Kahl, A.; Bauhus, J.; Wirth, C. Many ways to die—Partitioning tree mortality dynamics in a near-natural mixed deciduous forest. *J. Ecol.* **2013**, *101*, 220–230. [CrossRef]
28. Lines, E.; Coomes, D.; Purves, D. Influences of forest structure, climate and species composition on tree mortality across the eastern US. *PLoS ONE* **2010**, *5*, e13212. [CrossRef] [PubMed]
29. Muller-Landau, H.C.; Condit, R.S.; Chave, J.; Thomas, S.C.; Bohlman, S.A.; Bunyavejchewin, S.; Davies, S.; Foster, R.; Gunatilleke, S.; Gunatilleke, N.; et al. Testing metabolic ecology theory for allometric scaling of tree size, growth and mortality in tropical forests. *Ecol. Lett.* **2006**, *9*, 575–588. [CrossRef] [PubMed]
30. Hember, R.A.; Coops, N.C.; Kurz, W.A. Statistical performance and behaviour of environmentally-sensitive composite models of lodgepole pine growth. *For. Ecol. Manag.* **2018**, *408*, 157–173. [CrossRef]
31. Pokharel, B.; Dech, J.P. Mixed-effects basal area increment models for tree species in the boreal forest of Ontario, Canada using an ecological land classification approach to incorporate site effects. *Forestry* **2012**, *85*, 255–270. [CrossRef]
32. Corcuera, L.; Camarero, J.J.; Sisó, S.; Gil-pelegrín, E. Radial-growth and wood-anatomical changes in overaged *Quercus pyrenaica* coppice stands: Functional responses in a new Mediterranean landscape. *Trees* **2006**, *20*, 91–98. [CrossRef]
33. Pellizzari, E.; Camarero, J.J.; Gazol, A.; Sangüesa-Barreda, G.; Carrer, M. Wood anatomy and carbon-isotope discrimination support long-term hydraulic deterioration as a major cause of drought-induced dieback. *Glob. Chang. Biol.* **2016**, *22*, 2125–2137. [CrossRef] [PubMed]
34. Ryan, M.; Binkley, D.; Fownes, J. Age-related decline in forest productivity: Pattern and process. *Adv. Ecol. Res.* **1997**, *27*, 213–262.
35. Ryan, M.G.; Phillips, N.; Bond, B.J. The hydraulic limitation hypothesis revisited. *Plant Cell Environ.* **2006**, *29*, 367–381. [CrossRef] [PubMed]
36. Norby, R.; Luo, Y. Evaluating ecosystem responses to rising atmospheric CO_2 and global warming in a multi-factor world. *New Phytol.* **2004**, *162*, 281–293. [CrossRef]
37. Landsberg, J. Modelling forest ecosystems: State of the art, challenges, and future directions. *Can. J. For. Res.* **2003**, *33*, 385–397. [CrossRef]
38. Liu, J.; Ashton, P.S. Individual-based simulation models for forest succession and management. *For. Ecol. Manag.* **1995**, *73*, 157–175. [CrossRef]
39. Monserud, R.A. Evaluating forest models in a sustainable forest management context. *For. Biometry Model. Inf. Sci.* **2003**, *1*, 35–47.
40. Weiskittel, A.R.; Hann, D.W.; Kershaw, J.A.; Vanclay, J.K. Tree-Level Models. In *Forest Growth and Yield Modeling*; John Wiley & Sons, Ltd.: Hoboken, NJ, USA, 2011; pp. 69–84. [CrossRef]
41. Lambert, M.C.; Ung, C.H.; Raulier, F. Canadian national tree aboveground biomass equations. *Can. J. For. Res.* **2005**, *35*, 1996–2018. [CrossRef]
42. Ung, C.; Bernier, P.; Guo, X. Canadian national biomass equations: New parameter estimates that include British Columbia data. *Can. J. For. Res.* **2008**, *38*, 1123–1132. [CrossRef]
43. Lamlom, S.H.; Savidge, R.A. A reassessment of carbon content in wood: Variation within and between 41 North American species. *Biomass Bioenergy* **2003**, *25*, 381–388. [CrossRef]
44. Fortin, M.; DeBlois, J. Modeling Tree Recruitment with Zero-Inflated Models: The Example of Hardwood Stands in Southern Québec, Canada. *For. Sci.* **2007**, *53*, 529–539.
45. Lexerød, N.L. Recruitment models for different tree species in Norway. *For. Ecol. Manag.* **2005**, *206*, 91–108. [CrossRef]
46. Li, R.; Weiskittel, A.R.; Kershaw, J.A. Modeling annualized occurrence, frequency, and composition of ingrowth using mixed-effects zero-inflated models and permanent plots in the Acadian Forest Region of North America. *Can. J. For. Res.* **2011**, *41*, 2077–2089. [CrossRef]
47. Vanclay, J.K. Modelling regeneration and recruitment in a tropical rain forest. *Can. J. For. Res.* **1992**, *22*, 1235–1248. [CrossRef]

48. Coops, N.C.; Waring, R.H. Estimating the vulnerability of fifteen tree species under changing climate in Northwest North America. *Ecol. Model.* **2011**, *222*, 2119–2129. [CrossRef]
49. McKenney, D.W.; Pedlar, J.H.; Lawrence, K.; Campbell, K.; Hutchinson, M.F. Potential Impacts of Climate Change on the Distribution of North American Trees. *BioScience* **2007**, *57*, 939–948. [CrossRef]
50. Nitschke, C.R.; Innes, J.L. A tree and climate assessment tool for modelling ecosystem response to climate change. *Ecol. Model.* **2008**, *210*, 263–277. [CrossRef]
51. Worrall, J.J.; Rehfeldt, G.E. Recent declines of *Populus tremuloides* in North America linked to climate. *For. Ecol. Manag.* **2013**, *299*, 35–51. [CrossRef]
52. Monserud, R.A.; Sterba, H. A basal area increment model for individual trees growing in even- and uneven-aged forest stands in Austria. *For. Ecol. Manag.* **1996**, *80*, 57–80. [CrossRef]
53. Pretzsch, H.; Biber, P. Size-symmetric versus size-asymmetric competition and growth partitioning among trees in forest stands along an ecological gradient in central Europe. *Can. J. For. Res.* **2010**, *40*, 370–384. [CrossRef]
54. Woods, A.J.; Heppner, D.; Kope, H.H.; Burleigh, J.; Maclauchlan, L. Forest health and climate change: A British Columbia perspective. *For. Chron.* **2010**, *86*, 412–422. [CrossRef]
55. Kurz, W.A.; Dymond, C.C.; White, T.M.; Stinson, G.; Shaw, C.H.; Rampley, G.J.; Smyth, C.; Simpson, B.N.; Neilson, E.T.; Trofymow, J.A.; et al. CBM-CFS3: A model of carbon-dynamics in forestry and land-use change implementing IPCC standards. *Ecol. Model.* **2009**, *220*, 480–504. [CrossRef]
56. Li, Z.; Kurz, W.; Apps, M.; Beukema, S. Belowground biomass dynamics in the Carbon Budget Model of the Canadian Forest Sector: Recent improvements and implications for the estimation of NPP and NEP. *Can. J. For. Res.* **2003**, *33*, 126–136. [CrossRef]
57. Wooldridge, J.M. *Introductory Econometrics: A Modern Approach*, 5th ed.; South-Western Cengage Learning: Mason, OH, USA, 2013.
58. Stinson, G.; Kurz, W.A.; Smyth, C.E.; Neilson, E.T.; Dymond, C.C.; Metsaranta, J.M.; Boisvenue, C.; Rampley, G.J.; Li, Q.; White, T.M.; et al. An inventory-based analysis of Canada's managed forest carbon dynamics, 1990 to 2008. *Glob. Chang. Biol.* **2011**, *17*, 2227–2244. [CrossRef]
59. Trofymow, J.; Stinson, G.; Kurz, W. Derivation of a spatially explicit 86-year retrospective carbon budget for a landscape undergoing conversion from old-growth to managed forests on Vancouver Island, BC. *For. Ecol. Manag.* **2008**, *256*, 1677–1691. [CrossRef]
60. Sankarasubramanian, A.; Vogel, R.M.; Limbrunner, J.F. Climate elasticity of streamflow in the United States. *Water Resour. Res.* **2001**, *37*, 1771–1781. [CrossRef]
61. Taylor, T.; Greenlaw, S. Elasticity. In *Principles of Economics*; OpenStax College: Houston, TX, USA, 2014; Chapter 5; pp. 99–113.
62. Oliver, C.; Larson, B. *Forest Stand Dynamics*, 1st ed.; John Wiley and Sons: New York, NY, USA, 1996.
63. Bormann, F.; Likens, G. Catastrophic disturbance and the steady-state in northern hardwood forests. *Am. Sci.* **1979**, *67*, 660–669.
64. Whittaker, R.H.; Likens, G.E. Primary production: The biosphere and man. *Hum. Ecol.* **1973**, *1*, 357–369. [CrossRef]
65. Wullschleger, S.D.; Post, W.M.; King, A.W. On the potential role for CO_2 fertilization effect in forests: Estimates of the biotic growth factor based on 58 controlled-exposure studies. In *Biotic Feedbacks in the Global Climatic System: Will the Warming Feed the Warming?* Woodwell, G.M., Mackenzie, F.T., Eds.; Oxford University Press: New York, NY, USA, 1995.
66. Allen, C.D.; Macalady, A.K.; Chenchouni, H.; Bachelet, D.; McDowell, N.; Vennetier, M.; Kitzberger, T.; Rigling, A.; Breshears, D.D.; Hogg, E.H.; et al. A global overview of drought and heat-induced tree mortality reveals emerging climate change risks for forests. *For. Ecol. Manag.* **2010**, *259*, 660–684. [CrossRef]
67. Peng, C.; Ma, Z.; Lei, X.; Zhu, Q.; Chen, H.; Wang, W.; Liu, S.; Li, W.; Fang, X.; Zhou, X. A drought-induced pervasive increase in tree mortality across Canada's boreal forests. *Nat. Clim. Chang.* **2011**, *1*, 467–471. [CrossRef]
68. Van Mantgem, P.J.; Stephenson, N.L.; Byrne, J.C.; Daniels, L.D.; Franklin, J.F.; Fule, P.Z.; Harmon, M.E.; Larson, A.J.; Smith, J.M.; Taylor, A.H.; et al. Widespread increase of tree mortality rates in the Western United States. *Science* **2009**, *323*, 521–524. [CrossRef] [PubMed]

69. Bennett, A.C.; McDowell, N.G.; Allen, C.D.; Anderson-Teixeira, K.J. Larger trees suffer most during drought in forests worldwide. *Nat. Plants* **2015**, *1*, 15139. [CrossRef] [PubMed]
70. D'Amato, A.W.; Bradford, J.B.; Fraver, S.; Palik, B.J. Effects of thinning on drought vulnerability and climate response in north temperate forest ecosystems. *Ecol. Appl.* **2013**, *23*, 1735–1742. [CrossRef] [PubMed]
71. Fernández-de-Uña, L.; Cañellas, I.; Gea-Izquierdo, G. Stand Competition Determines How Different Tree Species Will Cope with a Warming Climate. *PLoS ONE* **2015**, *10*, e0122255. [CrossRef] [PubMed]
72. Young, D.J.N.; Stevens, J.T.; Earles, J.M.; Moore, J.; Ellis, A.; Jirka, A.L.; Latimer, A.M. Long-term climate and competition explain forest mortality patterns under extreme drought. *Ecol. Lett.* **2017**, *20*, 78–86. [CrossRef] [PubMed]
73. Zang, C.; Pretzsch, H.; Rothe, A. Size-dependent responses to summer drought in Scots pine, Norway spruce and common oak. *Trees* **2012**, *26*, 557–569. [CrossRef]
74. Flannigan, M.; Amiro, B.; Logan, K.; Stocks, B.; Wotton, B. Forest fires and climate change in the 21st century. *Mitig. Adapt. Strateg. Glob. Chang.* **2006**, *11*, 847–859. [CrossRef]
75. Woods, A.J.; Coates, K.D.; Watts, M.; Foord, V.; Holtzman, E.I. Warning Signals of Adverse Interactions between Climate Change and Native Stressors in British Columbia Forests. *Forests* **2017**, *8*, 280. [CrossRef]